Discrete forms of Mössbauer spectra

A. M. Afanas'ev

Physicotechnical Institute of the Russian Academy of Sciences, 117218 Moscow, Russia

M. A. Chuev

Russian Scientific Center "Kurchatov Institute" 123182 Moscow, Russia

A new method is proposed for analyzing Mössbauer spectra, which allows models of the spectra to be found with the largest possible number of lines. The technique is based on the proposition that for any given level of measurement accuracy it is impossible to detect splitting of the lines which is too small. Formulated mathematically, this allows certain criteria to be established on the density of the lines over the spectrum, by means of which the spectral model is not described in advance but is derived directly by fitting. The possibilities inherent in the method are demonstrated using examples of Mössbauer spectra for high-temperature superconductors. © *1995 American Institute of Physics.*

1. INTRODUCTION

Mössbauer spectroscopy is a powerful technique for deriving information about the properties of solid bodies from the hyperfine interactions of the Mössbauer nucleus with internal electrical and magnetic fields. The experimental method allows measurements to be made with high precision, but extracting the parameters of the hyperfine structure requires a corresponding mathematical processing which should be commensurate with the capability of the experiment.

The existing methods for fitting spectra can be divided into two classes. When the number of lines is relatively small the χ^2 method is used, i.e., the method of least squares.[1-3] In alloys and amorphous materials a large number of lines from nonequivalent Mössbauer ion states can be superposed, and it is necessary to introduce continuous distributions of hyperfine fields and to analyze them using a large number of lines, comparable with the number of spectral points. It is well known that this procedure leads to an ill-posed problem, and a large number of treatments have been devoted to it.[4-8]

Without going into the mathematical nuances of these approaches, we note an important difference between them. In the χ^2 method the aim of the analysis is to extract the spectral parameters along with an indication of their precision, i.e., an indication of the root-mean-square error. In the second approach there is actually no quantitative information in the sense that it contains no procedure for determining the errors of the parameters deduced. More careful examination reveals that the χ^2 method in many cases is also not quantitative. The procedure for determining the errors in the χ^2 method is feasible only when a model of the structure, i.e., the number of lines in the spectrum is known exactly. In general this information is not known *a priori*, and it is necessary to use approximate models, which in some situations are quite crude.

There exist mathematical methods for determining the reliability of these models, but the applicable criteria for reliability are quite stringent—it is necessary that the χ^2 pa-

rameter be very close to unity, which in many cases is not true. Naturally, in such cases the question of the precision of the resulting parameters remains open.

In the present work we consider the problem of finding spectral models with the largest possible number of lines, but which allow a quantitative description with an indication of the average values and the errors in the derived parameters. The method is based on the idea that at a given level of measurement precision it is impossible to specify lines with too small a separation. This idea, formulated mathematically, enables us to establish an upper limit on the line number density even before the fitting procedure is carried out, and also to combine two lines into one according to certain criteria during the fitting process. Thus, the model is not prescribed ahead of time, but is derived directly in the course of fitting the spectrum. The basis of the method is described in Sec. 2.

Generally speaking, the resulting solutions contain a large number of lines, and they may be quite difficult to interpret. The solutions can be simplified by throwing out lines with low intensities, combining closely spaced lines and by imposing relationships and using certain models about the shape of individual lines. These questions are discussed in Sec. 3 using spectra of high-temperature superconductors (HTSC) as examples.

2. STATEMENT OF THE PROBLEM AND FUNDAMENTAL IDEAS OF THE THEORY

A Mössbauer absorption spectrum consists of a convolution of the line $L_s(v)$ of the source and the spectrum $F_a(v)$ of the absorber:

$$F(v) = L_s(v) * F_a(v) + B = \int L_s(v - v_1) F_a(v_1) dv_1 + B. \tag{1}$$

Here B is the number of photons which pass far from resonance. The function $L_s(v)$ is defined by the natural line width Γ_0 and the density of the line distribution $\rho_s(v)$ in the source:

$$L_s(v) = f_s \frac{\Gamma_0}{2\pi} \int \frac{\rho_s(x)dx}{(v-x)^2 + (\Gamma_0/2)^2}, \qquad (2)$$

where f_s is the probability of the Mössbauer effect in the source.

The spectrum of the absorber is defined by the following expression:

$$F_a(v) = 1 - \exp\left(-\alpha \frac{\Gamma_0^2}{4} \int \frac{\rho_a(x)dx}{(v-x)^2 + (\Gamma_0/2)^2}\right). \qquad (3)$$

Here $\rho_a(x)$ is the density of the line distribution in the absorber and $\alpha = f_a n_a \sigma_0 t$ is the effective width of the absorber, f_a is the probability of the Mössbauer effect in the absorber, n_a is the density of resonant nuclei in the absorber, σ_0 is the transverse resonant absorption cross section, and t is the thickness of the absorber. In the case of a "thin" absorber ($\alpha \ll 1$) and a source with a single line we have

$$F(v) = f_s \alpha \frac{\Gamma}{2\pi} \int \frac{\rho_a(x)dx}{(v-x)^2 + (\Gamma/2)^2} + B, \qquad (4)$$

where $\Gamma = 2\Gamma_0$ is twice the natural line width.

The experimental spectrum $N(v_i)$ is measured at a finite number n of points v_i and contains statistical noise ξ_i, so that

$$N(v_i) = F(v_i) + \xi_i. \qquad (5)$$

It is assumed that the noise ξ is uncorrelated, i.e.,

$$\langle \xi_i \xi_j \rangle = \sigma_i^2 \delta_{ij} = N(v_i)\delta_{ij}. \qquad (6)$$

Usually the density $\rho_a(x)$ of the lines in the absorber is prescribed in the form of a finite number n_l of lines of a certain form:

$$\rho_a(x) = \sum_{k=1}^{n_l} \alpha_k f_k(x - \delta_k). \qquad (7)$$

Here α_k determines the intensity and δ_k the rotations of the lines. The individual line shapes are usually given by Lorentzians:

$$L_1(x, \gamma_k) = \frac{\gamma_k}{2\pi} \frac{1}{x^2 + (\gamma_k/2)^2},$$

where γ_k is the line width. The regular part of the spectrum is represented in the form

$$F(v_i) = \sum_{k=1}^{n_l} A_k L_1(v_i - \delta_k, \Gamma_k) + B, \qquad (8)$$

where $\Gamma_k = \Gamma + \gamma_k$ and $A_k = f_s \alpha \alpha_k$.

2.1. Method of least squares

In the method of least squares the unknown parameters A_k, δ_k, Γ_k, and B are found by minimizing the functional

$$\chi^2 = \frac{1}{n - n_p} \sum_{i=1}^{n} \frac{1}{\sigma_i^2} [N(v_i) - F(v_i)]^2, \qquad (9)$$

where $n_p = 3n_l + 1$ is the number of unknown parameters. The problem reduces to solving the system of nonlinear equations:

$$\partial \chi^2 / \partial \beta_j = 0, \qquad (10)$$

where β_j is one of the parameters A_k, δ_k, Γ_k, B. From the solution of the system (10) the average values $\bar\beta_j$ are found, where the matrix of second derivatives

$$G_{qk} = \sum_{i=1}^{n} \frac{1}{\sigma_i^2} \frac{\partial F(v_i)}{\partial \beta_q} \frac{\partial F(v_i)}{\partial \beta_k} \qquad (11)$$

determines the mean square errors:

$$\langle \Delta \beta_k \Delta \beta_q \rangle = G_{qk}^{-1}. \qquad (12)$$

The quantity χ^2 defined by Eq. (9) is used in statistical analysis not only as the functional to be minimized in the technique for estimating the parameters β_k, but also as a statistic which allows one to determine the quality of the fit or to choose the most optimum model if several ways of describing the spectrum are available.[1,9]

The parameter χ^2 is a random quality with the distribution $\chi^2(r)$, which asymptotically approaches a normal distribution when the number of degrees of freedom $r = n - n_p$ is large.[9] The normalizing coefficient $1/(n-n_p)$ in (9) is chosen so that when the method of estimating (10) is employed we have $\bar\chi^2 = 1$ in the limit of large r. Then the mean square deviation of χ^2 from unity is

$$\Delta \chi^2 = \sqrt{2/(n - n_p)}. \qquad (13)$$

2.2. Limitations on the density with which lines are distributed through the spectrum

The χ^2 method is the best fitting procedure when the number of lines is known, but here the number of lines is not known in advance. It would seem that there is a simple way out of the situation: choose the largest possible number of lines, e.g., equal to the number of channels. In this case there is a simple mathematical solution, but because of the statistical noise this solution turns out to be inappropriate from the physical standpoint: lines appear with negative intensities, etc. (see Fig. 1b). This problem is well known to be ill-posed.[10] In order to obtain reasonable solutions restrictions on the form of the distributions are introduced by introducing auxiliary terms in the functional (9). Thus, in Ref. 4 a functional was used which restricted the variations of the intensities A_k in neighboring channels:

$$u = \chi^2 + \lambda \sum_{k=2}^{n_l} (2A_k - A_{k-1} - A_{k+1}). \qquad (14)$$

By varying the parameter λ we can find solutions without negative intensities (see Fig. 1c). The form of the smoothing term is not unique, however, and Ref. 8 used the functional

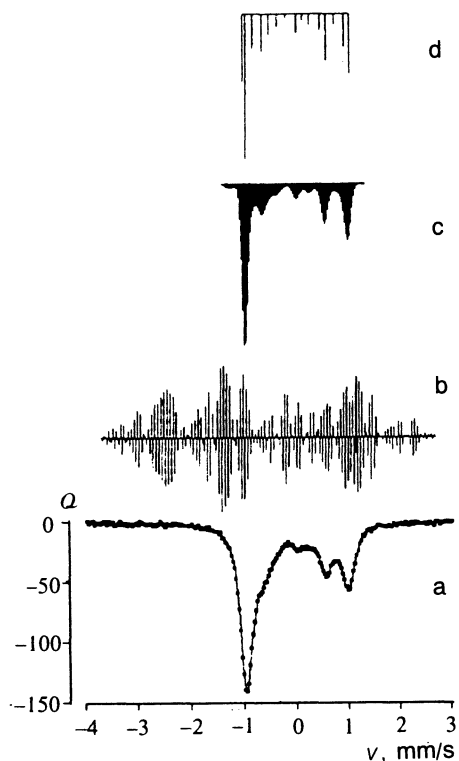$$u = \chi^2 + \lambda \sum_{k=1}^{n_l} A_k \ln A_k. \qquad (15)$$

FIG. 1. Mössbauer absorption spectrum (a) for ^{57}Fe nucleus in oriented polycrystalline samples of the HTSC $YBa_2(Cu_{.95}Fe_{.05})_3O_{6.8}$ for an angle between the axis and the γ-ray beam of $\theta=0°$ and various models of the line distribution: b) equivalently positioned lines ($\chi^2=1.21$); c) Hesse–Rubartsch technique ($\chi^2=1.35$); d) "densest possible" solution in the present technique ($\chi^2=1.02$); here Q is the signal-to-noise ratio.

The formal similarity of the second term to the expression for the entropy is what permits this approach to be classified as a so-called maximum entropy formalism.

Another approach to the solution of the ill-posed problem is possible. The basic idea is that the number of allowed components in the spectrum should depend on the quality of the spectrum, i.e., on the signal-to-noise ratio. The occurrence of unphysical solutions in the example shown in Fig. 1 in an attempt to describe the spectrum with a large number of lines is due to the unreasonableness of the initial formulation of the problem: too large a number of fitting parameters was used.

In choosing a model we should first of all take into account the quality of the spectrum, and starting from that we should exclude solutions with unphysical behavior insofar as is possible. Let us analyze this concept for a simple example. Figure 2 shows model spectra of two closely separated lines (q is the separation between them) with different signal-to-noise ratios Q, together with the results of fitting the spectra in models with one and two lines (model 1 and model 2, respectively). For the spectrum with large Q the results of the fit unequivocally support the model with two lines, whereas for the spectrum with the small value of Q the χ^2 parameters are close to one another and it is not possible to make a convincing choice of one or the other model. Moreover, for this spectrum the description using two lines leads to a very large spread in the resulting parameters: the errors in determining A_1, A_2, and q are found to be larger than their mean values (see Table I). The use of model 2 in this case does not introduce any additional reliable information whatever. In general, for arbitrary Q the criterion for the reasonableness of model 2 is that the error in the intensity of each line be less than its mean value.

In choosing models of more complicated spectra we should exclude lines that do not satisfy the condition
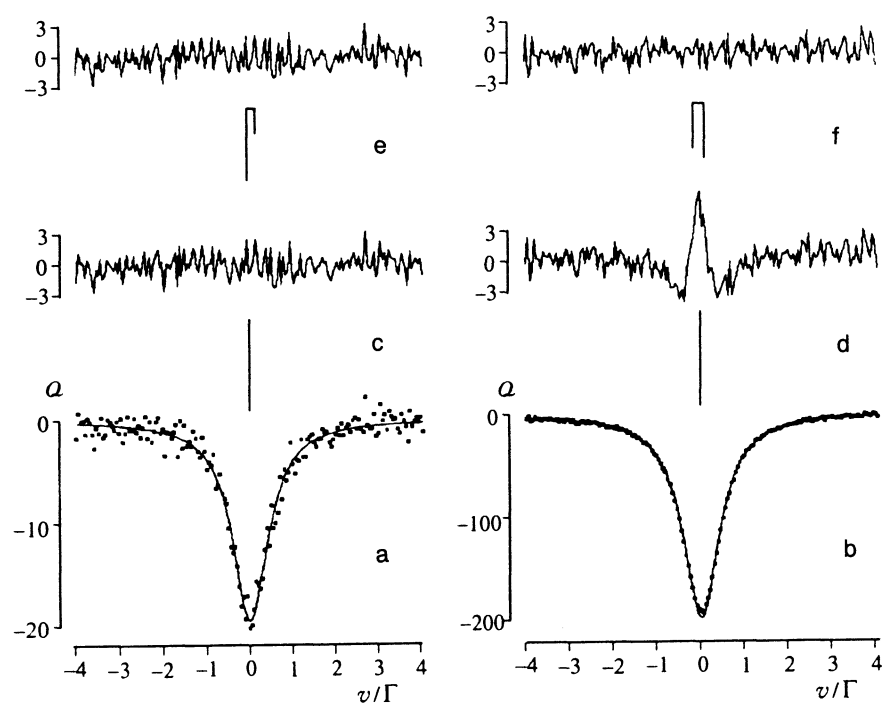
$$\Delta A_i < A_i.\tag{16}$$

FIG. 2. Model spectra of the line doublet ($q/\Gamma=.02$) with $Q=20$ (a) and 200 (b); the curves show the deviation between the model spectra and that calculated using one (c,d) and two (e,f) lines.

A. M. Afanas'ev and M. A. Chuev   562

TABLE I. Parameters of the spectra shown in Fig. 2.

	Spectrum a ($Q = 20$)		Spectrum b ($Q = 200$)	
	Model 1	Model 2	Model 1	Model 2
A_1	-	461(500)	-	2843(500)
A_2	-	161(500)	-	3454(500)
A	612(10)	621(10)	6197(10)	6296(20)
δ_1	-	-0.05(10)	-	-0.12(2)
δ_2	-	0.16(30)	-	0.09(2)
δ	0.003(9)	0.002(10)	0.0010(5)	0.0010(5)
q	-	0.21(20)	-	0.207(7)
χ^2	0.937	0.934	2.93	1.03

Note: A_i and δ_i are the intensity and position of the ith line; A is the toal intensity; δ is the center of mass of the two lines; q is the separation between the lines. The quantities δ_i, δ, and q are given in units of Γ. Errors are shown in parentheses.

In the models considered above we can find simple analytical expressions for the mean square errors of the derived parameters. Thus, for model *1* we have

$$\Delta A/\sqrt{2}A = \Delta\delta/\Gamma = \Delta\Gamma/\Gamma = 1/\bar{Q}, \qquad (17)$$

where we have written $\bar{Q} = \sqrt{2/\pi\Gamma}A$; here and in what follows Γ is the line width in the channels.

In real situations the parameter $\bar{Q}$ can reach a value of order 10^3, and consequently the precision with which the position of a line is determined can be very high.

For model 2 (see Appendix) the presence of a neighboring line (regardless of its intensity) increases the error in the intensity of each line, so that condition (16) is violated as soon as the separation q between lines becomes less than a quantity q_0, the solution of the equation

$$q_0 = (2/3)^{1/6} f_1(q_0)^{1/6}/\bar{Q}_i^{1/3}. \qquad (18)$$

For $q_0 \ll \Gamma$ this equation assumes the following simple form:

$$q_0 = \left(\frac{2}{3}\right)^{1/6}\frac{1}{\bar{Q}_i^{1/3}}. \qquad (19)$$

The presence of additional lines can only cause q_0 to increase, and so Eqs. (18) and (19) determine a lower bound on the separation between neighboring lines in spectra of the most general type. The parameters $\bar{Q}_i$ appearing in Eq. (18) are unknown. Exact knowledge of them, or what is the same thing, exact knowledge of the line intensities of the spectrum would amount to a complete solution of the original problem of fitting the spectrum. Consequently, in the initial stage of the analysis we can hope to obtain only more or less effective estimates for $\bar{Q}_i$.

If we express the experimental spectrum in units of the statistical error σ, which we will assume to be the same for all points of the spectrum, then the function

$$\overline{N(v_i)} = \sqrt{\frac{\pi\Gamma}{2}}\frac{N(v_i)}{\sigma} \qquad (20)$$

will immediately determine an upper bound for $\bar{Q}_i$, since the spectral line number density is bounded by the function

$$n_l(v_i) = 1/q_0 = a(\overline{N(v_i)}^{1/3})/\Gamma, \qquad (21)$$

where $a = (3/2)^{1/6} \approx 1.07$.

If the number of lines $N_l(\Gamma)$ over a portion of the spectrum of width Γ is much greater than unity, then the estimate (21) can be improved:

$$n_l(v_i) = 1/q_0 = a_1\overline{N(v_i)}^{1/4}/\Gamma, \qquad (22)$$

where $a_1 \approx 1.19$.

If the lines satisfy condition (16) and Eq. (22), then the total number of lines with which the analysis must start turns out to be much less than the number of channels, and the unphysical aspects of the solution are largely removed. However, the estimates of $\bar{Q}_i$ given above are not optimal and can be improved considerably.

2.3. Estimates of the line density over sharpened spectra

In Ref. 11 a new spectral sharpening technique was proposed which uses a simple transformation to derive new representations of the experimental data in which spectral line broadening due to the natural width of the lines of the source and the absorber is largely eliminated.

In accordance with (4) and (5), the regular part of the spectrum is a convolution of the spectral density $\rho_a(x)$ with a Lorentzian. Using the integral transformation

$$Af(v) = \frac{1}{2\pi}\int \frac{2f(v)-f(v-y)-f(v+y)}{y^2}\, dy, \qquad (23)$$

we can easily derive the peak spectrum:[11]

$$N_2(v) = N(v) + (\Gamma/2)AN(v)$$

$$= \frac{\Gamma^3}{4\pi}\int \frac{\rho_a(x)dx}{[(v-x)^2+(\Gamma/2)^2]^2} + \xi_2, \qquad (24)$$

which is a convolution of the spectral density $\rho_a(x)$ and the square of the Lorentzian. Successive application of the operator A allows us to obtain even higher orders of sharpening:

$$N_3(v) = N_2(v) + (\Gamma/6)A[N_2(v)-N(v)]$$

$$= \frac{\Gamma^5}{12\pi}\int \frac{\rho_a(x)dx}{[(v-x)^2+(\Gamma/2)^2]^3} + \xi_3, \qquad (25)$$

and so forth [cf. Eq. (11)]. The functions ξ_2 and ξ_3, which are transformations of the statistical noise ξ, are no longer white noise, i.e., they do not satisfy condition (6).

The sharpened spectrum $N_3(v)$ corresponding to the spectrum in Fig. 1a is shown in Fig. 3a; it more adequately represents the absorber line spectrum, and consequently determines the upper bound for $\bar{Q}_i$ more precisely than the original spectrum:

$$\bar{Q}_i < \bar{Q}_{3i} = \frac{3}{8}\overline{N_3(v_i)}. \qquad (26)$$

If we assume $N_1(\Gamma) \gg 1$, then in analogy with (22) we have

$$n_l(v_i) = 1/q_0 = a_3\overline{N_3(v_i)}^{1/4}/\Gamma, \qquad (27)$$

where $a_3 \approx 1.42$.

2.4. Method of least squares with combination of closely spaced lines

At the beginning of the fit the lines are arranged in accordance with condition (27). The first line is placed at the spectral point v_j with minimum value $N(v_i)$. The range of values around v_j within which there should be no lines is
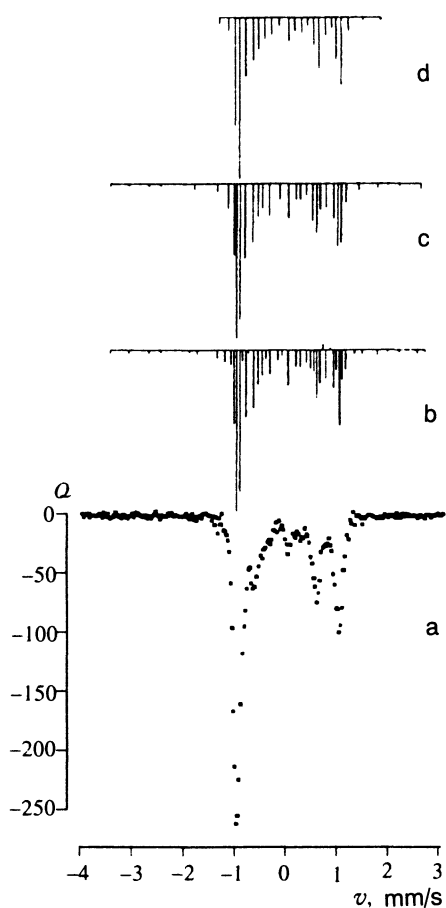
FIG. 3. Successive discrete forms of the spectrum in Fig. 1a: a) sharpened spectra; b) taking into account the limit on the line distribution density over the spectrum ($n_l=45$, $\chi^2=0.97$; c) after combining closely-spaced lines without changing their positions ($n_l=33$, $\chi^2=1.11$); d) base solution with the line positions varied ($n_l=23$, $\chi^2=1.01$).

FIG. 4. Potassium ferrocyanide calibration spectrum.

estimated according to Eq. (27), and this range is excluded from further consideration. The procedure is repeated until the whole range of velocities is exhausted. The resulting set of line positions is fixed and the χ^2 method is used to find the line intensities of these locations. Figure 3b shows the result of this analysis, from which it follows that even in this initial stage of the fit physically unacceptable aspects of the solution are substantially eliminated: there are few lines with negative intensities, their intensities are small in absolute value, and their total contribution to the spectrum is relatively small. Since the estimates (26) and (27) are approximate, in the solution shown in Fig. 3b some of the lines have large errors in the intensities, and condition (16) does not hold for them. Such lines are eliminated from further consideration by combining them with their neighbors which have higher uncertainties in intensity. Thus the intensity of the resulting line is defined as the sum of the intensities and its position is defined as the position of the center of mass of the combined lines. This procedure allows us to substantially reduce the number of lines (see Fig. 1c) without going through a complicated iteration procedure.

The next stage of analysis consists of fitting the spectrum using the χ^2 method, but now with both the intensities
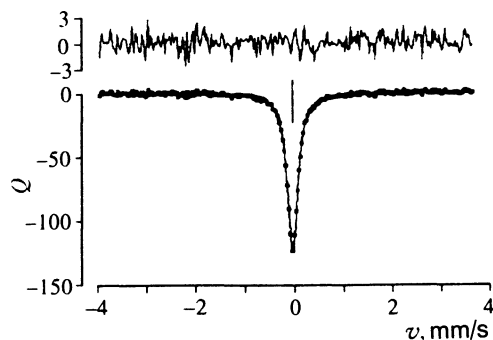
and the positions of the lines being varied. The spectral model found previously is used as a zeroth approximation. In the course of iteration lines can appear with large errors in the intensities, which are eliminated by combining two closely spaced lines exactly as described above.

Thus, in contrast to the dimensional χ^2 procedure, in this approach the number of lines in the model varies in the course of the spectral fit. Figure 3d shows the results of this analysis.

The analysis given illustrates the proposed alternative approach for solving ill-posed problems. The solution obtained, which can be defined as the base solution, is maximally allowed in the sense that it has the minimum value of χ^2 for the largest possible number of lines consistent with condition (16).

3. ANALYSIS OF THE BASE SOLUTION

The base solution found in the previous section is still not the final form of the density ρ_a of the absorber line distribution, since in a real experiment the Lorentzian form of the source line $L_s(v)$ undergoes distortion due to a different sort of interaction in the source itself, which can either cause additional broadening or change the shape of the line from Lorentzian. Although the additional broadening of the line in the source is generally small, the question regarding the line shape remains open and should be answered separately in each specific experiment by means of calibration measurements of the spectrum of a standard absorber. In our case a calibration spectrum of potassium ferrocyanide was measured; it approximates a Lorentzian line well with a width $\Gamma_k=0.244$ mm/s (Fig. 4). If we take into account the additional broadening in Eq. (4) and perform the analysis described in the previous section, we obtain the spectral model shown in Fig. 1d and in Table II. As can be seen, a relatively small amount of additional line broadening sharply reduces the number of lines in the model, which undoubtedly imposes severe demands on the behavior of the calibration measurements—the statistical quality of the calibration spectrum should be higher than for the spectrum of the sample being studied.

As can be seen from Table II, the fitting technique described above reveals lines of relatively low intensity (of order a few percent of the total area of the spectrum). Elimi-

TABLE II. Parameters of the model lines shown in Fig. 1d.

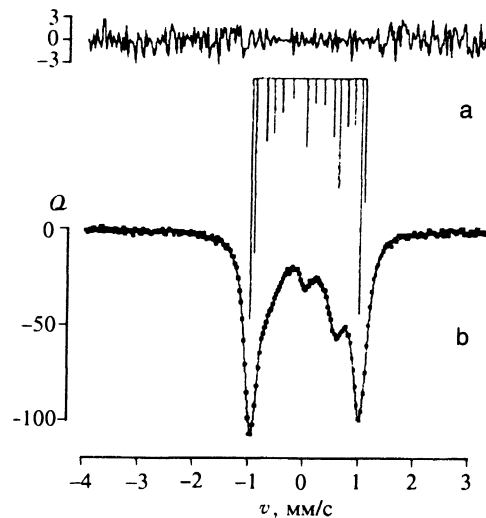| Line No.	Area, in %	Position in mm/s
1	13(7)	$-1.00(2)$
2	28(6)	$-0.94(1)$
3	7(1)	$-0.81(2)$
4	7.1(6)	$-0.63(1)$
5	3.9(6)	$-0.50(2)$
6	2.6(4)	$-0.37(3)$
7	0.7(4)	$-0.18(8)$
8	3.6(8)	$0.03(2)$
9	1.2(7)	$0.15(9)$
10	2.1(7)	$0.28(4)$
11	3(1)	$0.49(3)$
12	9(1)	$0.60(1)$
13	2.0(4)	$0.76(3)$
14	6(1)	$0.95(2)$
15	12(1)	$1.056(6)$

FIG. 5. Experimental spectrum (a) of the same HTSC sample as in Fig. 1a with a "magic" angle of incidence $\theta=55°$ and "densest possible" solution (b) for the spectrum.

nation of these lines increases χ^2, but this increase can be quite small, and if there is any difficulty in interpreting these lines they can be discarded in a first approximation. Thus, if we take away line 9 in the spectrum of Fig. 1d, then χ^2 increases by less than 0.001, and the question of whether this line exists or not can only be answered conclusively by means of more sensitive measurements.

We note two important features in the spectrum of Fig. 1d. First, not one additional line can be added to this spectrum without violating condition (16). Second, we can try to improve the agreement by varying the widths, but in this example that cannot be done without violating (16) and reducing the number of lines. Consequently, the model of Fig. 1d can be called the "densest possible" discrete solution for the spectrum of Fig. 1a.

The discrete forms of the spectrum found above approximate the real density of states, in which continuous line distributions may exist alongside the discrete lines. In general the form of these distributions is unknown and must be analyzed separately, but the most popular shape is a Gaussian distribution. The simplest way to test for the presence of continuous distributions using the technique described above is to combine two closely spaced lines into a single line of a particular shape (e.g., by convolving a Lorentzian and Gaussian line) whose width is an additional variable parameter. If the quantity χ^2 decreases as a result of adjustment, the assumption that there is a continuous distribution is confirmed. This procedure can be very useful, but in our specific example it is ineffective.

The maximum number of lines that can be resolved in the spectrum depends on the statistical quality of the spectrum. However, if some a priori information about the object of investigation is known which allows certain relations to be imposed on the parameters of the model, the number of permitted lines for a given level of statistics can be increased. As an example, consider the spectrum of the same oriented HTSC specimen measured in the geometry with a "magic" angle $\theta=55°$ between the axis and the γ-ray beam (Fig. 5a).

The densest possible model of fifteen lines for this spectrum obtained using the above technique is shown in Fig. 5b. However, in this geometry at an angle of incidence $\theta=55°$ the spectrum of the oriented specimen in the absence of magnetic hyperfine splitting should consist only of symmetric quadrupole doublets. In order to impose relationships we must use some intermediate spectrum with a large number of lines, e.g., the base model obtained without treating the additional broadening in the source, such as the model of Fig. 3d. The corresponding model consisting of twenty-one lines is shown in Fig. 6a.

Mössbauer studies of HTSCs have already been carried out for many years, and at the present time an extensive experimental data base has been compiled. For HTSC samples consisting of $YBa_2(Cu_{1-x}Fe_x)_3O_y$ with a low concentration $x<0.1$ of Fe and oxygen content $y \geqslant 6.5$ a large number of quadrupole doublets have been identified by various authors (see, e.g., Refs. 12–15 and work cited therein). These correspond to nonequivalent Fe atoms at Cu positions with a different configuration of nearest oxygen neighbors. The results of this work are summarized in Fig. 6b.

The imposition of relationships begins by combining the pair of the strongest lines in the model of Fig. 6a into a symmetric doublet installed in the diagram of Fig. 6b; then the spectrum is fitted again. The balancing procedure is repeated for the new set of parameters, and so on. After all the relationships are imposed, the spectrum is fitted using the additional broadening in the source. The resulting model, shown in Fig. 6c, now contains eighteen lines.

The line parameters in the models of the spectra of Figs. 1a and 5a can be made more precise if we take into account the fact that they are spectra of the same specimen, and perform a simultaneous analysis using lines at identical positions in both spectra. As an initial choice of the parameters it is natural to use the positions of the lines in the model of Fig. 6c, which contains a larger number of lines. The results of
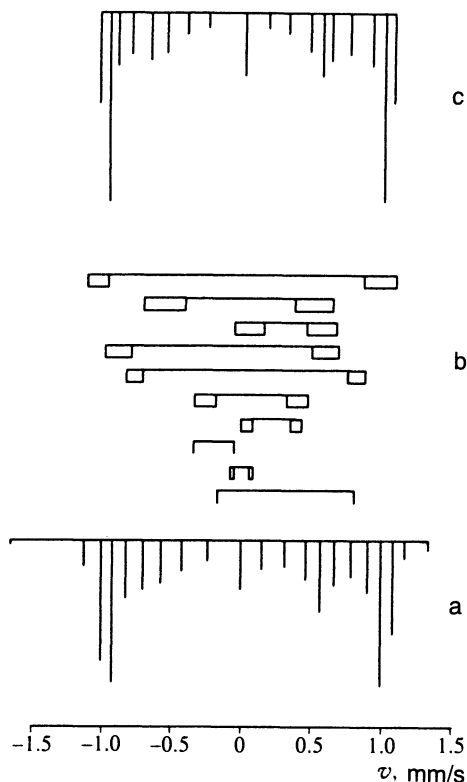
FIG. 6. Base model (a) and "densest possible" solution with relationships (c) for the spectrum of Fig. 5a; b) published data for the position of the quadrupole doublets in Mössbauer spectra of $YBa_2(Cu_{1-x}Fe_x)_3O_y$.

seen from Table III, the total line intensities in each doublet are the same within the limits of error for the two spectra, which argues in favor of the validity of this scheme of combining spectra into doublets.

These examples include the most important steps in the analysis that arises in the proposed new technique for fitting Mössbauer spectra.

4. CONCLUSION

Thus, in the present work an alternative approach has been proposed for solving ill-posed problems, based on the relatively simple principle that the line number density over a spectrum is limited by its statistical quality. The proposed procedure is uncomplicated to use and very efficient in terms of the number of numerical calculations, since there is no need to specify initial fitting parameters and a substantial portion of the analysis consists of verifying the criteria derived above, which does not require the use of an iterative procedure. The resulting model contains the largest possible number of lines that can be resolved in the spectrum with a given level of statistics, and it provides a good basis for further analysis.

The analysis carried out in this work of HTSC spectra, which are fairly complicated to interpret, gives reason to hope that the proposed technique may be efficiently used to solve a wide class of Mössbauer spectroscopy problems.

the fit are shown in Table III. Note that all the lines in the HTSC spectra identified in any previous work (see Fig. 6b) are shown in the resulting discrete version and are well determined in the sense that the errors in the intensity of all lines are less than their mean values. Furthermore, as can be

APPENDIX: MATRIX OF SECOND DERIVATIVES AND MEAN SQUARE ERRORS IN MODEL 2

For the model of a spectrum of two lines considered in Sec. 2.2 we introduce along with the intensities A_1 and A_2

TABLE III. Model line parameters in the combined analysis of the spectra of Figs. 1a and 5a.

Line No.	Area, in %		Position in mm/s
	Spectrum in Fig. 1a	Spectrum in Fig. 5a	
1	9(5)	9(4)	−1.01(1)
2	27(3)	18(3)	−0.95(1)
3	6(5)	5(3)	−0.90(2)
4	5.0(9)	4.0(5)	−0.80(1)
5	5.5(7)	4.6(6)	−0.66(2)
6	5.0(7)	3.8(6)	−0.54(2)
7	2.8(4)	2.1(3)	−0.40(2)
8	1.4(3)	1.5(3)	−0.24(2)
9	3.7(2)	6.2(2)	0.022(4)
10	1.9(3)	1.5(3)	0.19(2)
11	1.6(4)	2.1(3)	0.33(2)
12	2.0(7)	3.8(6)	0.48(2)
13	7(1)	6.2(2)	0.58(1)
14	3(1)	4.6(6)	0.64(1)
15	1.6(5)	4.0(5)	0.77(2)
16	3(2)	5(3)	0.93(3)
17	10(2)	18(3)	1.02(2)
18	5(2)	9(4)	1.09(2)

the dimensionless variables $y_{1,2} = \delta_{1,2}/\Gamma$ for the positions of the lines and the dimensionless parameter $q = (\delta_2 - \delta_1)/\Gamma$ which determines the separation between them.

Then the matrix of the second derivatives in (11) takes the following form:

$$G = \frac{1}{\pi\Gamma} \begin{pmatrix} 1 & \dfrac{1}{(1+q^2)} & 0 & -\dfrac{2A_2 q}{(1+q^2)^2} \\[2ex] \dfrac{1}{(1+q^2)} & 1 & \dfrac{2A_1 q}{(1+q^2)^2} & 0 \\[2ex] 0 & \dfrac{2A_1 q}{(1+q^2)^2} & 2A_1^2 & 2A_1 A_2 \dfrac{(1-3q^2)}{(1+q^2)^3} \\[2ex] -\dfrac{2A_2 q}{(1+q^2)^2} & 0 & 2A_1 A_2 \dfrac{(1-3q^2)}{(1+q^2)^3} & 2A_2^2 \end{pmatrix} . \tag{A1}$$

For the mean square errors we have, in accordance with (12),

$$\Delta A_1^2 = \Delta A_2^2 = \pi\Gamma \frac{1}{3q^6} f_1(q), \tag{A2}$$

$$\left(\frac{\Delta \delta_{1,2}}{\Gamma}\right)^2 = \frac{\pi\Gamma}{2A_{1,2}^2} \frac{1}{6q^4} f_2(q), \tag{A3}$$

where

$$f_1(q) = \frac{(1+q^2)^4 (30 + 6q^2 + 48q^4 + 45q^6 + 18q^8 + 3q^{10})}{30 + 107q^2 + 149q^4 + 108q^6 + 44q^8 + 10q^{10} + q^{12}}, \tag{A4}$$

$$f_2(q)$$

$$= \frac{(1+q^2)^6 (30 + 24q^2 + 6q^4)}{30 + 107q^2 + 149q^4 + 108q^6 + 44q^8 + 10q^{10} + q^{12}} .$$

In accordance with (A2), the errors $\Delta A_{1,2}$ for each of the lines increase without bound as $1/q^3$ when q decreases. On the other hand, the mean square error ΔA in the total intensity

$$\Delta A = \sqrt{6\pi\Gamma/5}, \tag{A5}$$

does not depend on q. A similar situation also arises in connection with the positions of the lines. The errors $\Delta\delta_{1,2}$ are proportional to $1/q^2$, whereas the mean square error in the position of the center of mass

$$\Delta\delta = \sqrt{\frac{5\pi\Gamma}{6}} \frac{\Gamma}{A}, \tag{A6}$$

is independent of q for small q. In deriving Eqs. (A5) and (A6) it is necessary to take into account the correlations in the errors of the intensities and positions of the lines:

$$\Delta A_1 \Delta A_2 = -\pi\Gamma \left(\frac{1}{3q^6} + \frac{2}{9q^4} + \frac{23}{54q^2} + \frac{91}{405}\right),$$

$$\left(\frac{\Delta\delta_1}{\Gamma}\right)\left(\frac{\Delta\delta_2}{\Gamma}\right) = \frac{\pi\Gamma}{2A_1 A_2}\left(\frac{1}{3q^4} + \frac{31}{45q^2}\right),$$

$$\Delta A_{1,2}\left(\frac{\Delta\delta_{1,2}}{\Gamma}\right) = \pm\frac{\pi\Gamma}{A_{1,2}}\left(\frac{1}{q^5} + \frac{5}{3q^3} + \frac{31}{90q}\right),$$

$$\Delta A_{1,2}\left(\frac{\Delta\delta_{2,1}}{\Gamma}\right) = \pm\frac{\pi\Gamma}{A_{2,1}}\left(\frac{1}{q^5} + \frac{5}{3q^3} + \frac{49}{90q}\right).$$

[1] W. T. Eadie, D. Drijard, F. E. James, M. Roos, and B. Sadoulet, *Statistical Methods in Experimental Physics*, Elsevier, New York (1971).
[2] C. Janot, *L'Effect Mossbauer et ses Applications*, Masson et Cie, Paris (1972).
[3] G. K. Shenoy and F. E. Wagner, *Mössbauer Isomer Shifts*, North-Holland, Amsterdam (1978).
[4] J. Hesse and H. Rubrtsch, J. Phys. E: Sci. Instrum. **7**, 526 (1974).
[5] P. Mangin, G. Marshal, M. Piecuch, and C. Janot, J. Phys. E: Sci. Instrum. **9**, 1101 (1976).
[6] G. Le Caer and J. M. Dubois, J. Phys. E: Sci. Instrum. **12**, 1083 (1979).
[7] C. Wivel and S. Morup, J. Phys. E: Sci. Instrum. **14**, 605 (1981).
[8] R. A. Brand and G. Le Caer, Nucl. Instrum. and Meth. B **34**, 272 (1988).
[9] H. Cramer, *Mathematical Methods of Statistics*, Princeton Univ. Press, Princeton, New Jersey (1946).
[10] A. N. Tikhonov and V. Ya. Arsenin, *Solution of Ill-Posed Problems*, Winston, Washington, DC (1977).
[11] A. M. Afanas'ev and E. Yu. Tsymbal, Hyperfine Interact. **62**, 325 (1990).
[12] R. A. Brand, Ch. Sauer, H. Lutgemeier *et al.*, Physica C **156**, 539 (1988).
[13] A. M. Afanas'ev, E. Yu. Tsymbal, V. M. Cherepanov *et al.*, Sol. State Commun. **76**, 701 (1990).
[14] S. Nasu, M. Yoshida, Y. Oda *et al.*, J. Magn. Magn. Mater. **90–91**, 664 (1990).
[15] V. Chechersky and A. Nath, Hyperfine Interact. **72**, 173 (1992).

Translated by David L. Book